International Journal of Physical Sciences

Volume 9 Number 22 30 November, 2014

ISSN 1992-1950

Academic Journals

ABOUT IJPS

The **International Journal of Physical Sciences (IJPS)** is published weekly (one volume per year) by Academic Journals.

International Journal of Physical Sciences (IJPS) is an open access journal that publishes high-quality solicited and unsolicited articles, in English, in all Physics and chemistry including artificial intelligence, neural processing, nuclear and particle physics, geophysics, physics in medicine and biology, plasma physics, semiconductor science and technology, wireless and optical communications, materials science, energy and fuels, environmental science and technology, combinatorial chemistry, natural products, molecular therapeutics, geochemistry, cement and concrete research, metallurgy, crystallography and computer-aided materials design. All articles published in IJPS are peer-reviewed.

Contact Us

Editorial Office: ijps@academicjournals.org

Help Desk: helpdesk@academicjournals.org

Website: http://www.academicjournals.org/journal/IJPS

Submit manuscript online http://ms.academicjournals.me/

Editors

Editorial Board

International Journal of Physical Sciences

Table of Contents: Volume 9 Number 22, 30 November, 2014

ARTICLES

academicJournals

Vol. 9(22), pp. 487-494, 30 November, 2014
DOI: 10.5897/IJPS2014.4187
ISSN 1992 - 1950
Article Number: 98D1AAE48839

http://www.academicjournals.org/IJPS

International Journal of Physical Sciences

Full Length Research Paper

Flat gravity based on Hubble's law which expanded Newtonian gravity

Shinsuke Hamaji

Hyama Natural Science Research Institute, 403 Daiichi-Kiriya, building 5-2, Chuo 2-chome, Nakano-ku, Tokyo 164-0011, Japan.

Received 16 July, 2014; Accepted 13 November, 2014

Hubble's law, formulated by Edwin Hubble and Milton Humason in 1929, tells us that space is expanding. However, over short distances, flat gravity caused by the expanding universe is described by the inverse square law of Newtonian gravity. This leads to heretofore unsolved gravity anomalies, such as the pioneer anomaly, which involves an abnormal slowdown relative to the Sun of the Pioneer spacecraft and the galaxy rotation problem, whereby the rotational speed of heavenly bodies reaches a constant value instead of decreasing with distance from the galactic centre. The expanding universe adds an expansion term that was divided into a strain constant V_0 for the recession rate $v = H_0D$, and the gravitational potential $-GM(1/r)$ of Newtonian mechanics for a stationary universe is replaced by $-GM(1/r)(1 + v/V_0)$. The expansion term becomes constant ($G_0 = GH_0/V_0$) at large distances because the distance D and radius r cancel. Furthermore, the total gravitational mass [$M_0 = c^3/(2GH_0)$] of the observable universe affects the specific potential constant, which is multiplied by the observable gravitational mass to become $-(G/r + G_0)M$. Flat gravity based on Hubble's law which expanded Newtonian gravity is thus consistent with the gravity anomaly without assuming the existence of dark matter. When combined with Yukawa potential [$\alpha e^{(-r/\lambda)}$], the gravity and the strong force can be unified [$\alpha e^{(-r/\lambda)} - 1](G/r + G_0)M$.

Key words: Expanding universe, inverse square law, pioneer anomaly, galaxy rotation problem, recession rate, gravitational potential, stationary universe, gravitational mass, specific potential, dark matter.

INTRODUCTION

Several physical problems in astronomy still remain open. One is the "Pioneer anomaly", which was noticed for the Pioneer 10 and 11 spacecrafts as they left the solar system. The anomaly involves the cause of the blueshift, which indicates a reduction in speed with respect to the sun and remains unidentified (Anderson et al., 1998). Another open problem is the "galaxy rotation problem" wherein the rotational speed of galactic matter does not decrease with distance from the galactic centre but remains constant (Zwicky, 1933, 1937). Neither of these problems can be explained by Newton's universal law of gravitation. Some theories have been proposed to revise Newton's law of gravity, such as modified Newtonian dynamics (MOND), which introduces a function that scales mass and that asymptotically approaches unity for accelerations greater than a constant acceleration defined

E-mail: s_hyama@yahoo.co.jp, Tel: +81-70-6611-3358. Fax: +81-70-6611-3358.

in the theory to be on the order of 10^{-10} m/s^2 (Milgrom, 1983). Another proposition is the modified gravitation theory (MOG), which expands the theory of general relativity and calls upon a fifth field of force to counteract gravity. However, this theory suggests that, because work becomes small at large distances, gravity must become relatively large, which would require the gravitational constant to change (Brownstein and Moffat, 2006). In addition, the dark-matter hypothesis invokes some unknown "dark" matter (that is, it does not emit radiation) that would account for the observed gravitational anomalies without requiring our current theory of gravity to be modified (Rubin et al., 1980). There is no rationale for the fifth field of force and dark matter remains undiscovered, so the debate is not settled. This paper approaches the problem by assuming an expanding universe, and that a gravitational interaction between all the observable gravitational mass of the universe is the cause of the gravity anomaly. Given this, the spatiotemporal evolution factor from Hubble's law was first defined (Hubble, 1929) and from this the pioneer anomaly and the galaxy rotation problem was explained.

METHODS

Given these relationships, the gravity anomalies by using the specific potential and the equivalence principle of light's momentum (LEP) was examined.

Definition of specific potential

Consider the equation $v = H_0D$, where v is the speed (that is, recession rate) at which heavenly bodies move away from an observer and D is the distance from the observer to the heavenly bodies. The proportionality constant H_0 is the Hubble constant and determines the recession rate of the current universe. As of 2013, the most accurate value for the Hubble constant, which comes from the Planck observation, is 67.80 ± 0.77 km/s/Mpc (Ade et al., 2013). This recession rate is divided into the recession strain constant V_0 (m/s) and is converted into the recession strain e for the cosmic expansion:

$$e = \frac{v}{V_0} = \frac{H_0 D}{V_0}. \tag{1}$$

The relationship between the recession strain e and the recession stretch Λ is

$$\Lambda = 1 + e = 1 + \frac{H_0 D}{V_0}. \tag{2}$$

These equations are expressed by using the ratio of the transformation of the initial state of the spatiotemporal evolution. In addition, we must ask if the recession of galaxies (due to cosmic expansion), and the existence of recession strain and stretch where no expansion occurs are valid before and after unification. Consider the specific potential G_x obtained by multiplying the recession stretch by the gravitational constant and dividing the product by distance:

$$G_x = \frac{\Lambda G}{D} = \frac{G}{D} + \frac{GH_0}{V_0}\,\mathrm{m^2 s^{-2} kg^{-1}}. \tag{3}$$

The specific potential G_x (J/kg^2) multiplied by the active gravitational mass M_a (kg) gives the potential G_xM_a (J/kg). The potential G_xM_a (J/kg) multiplied by the passive gravitational mass m_p (kg) gives the potential energy $G_xM_am_p$ (J). To obtain the specific potential constant G_0, the Hubble constant was multiplied by the gravitational constant and the product divided by the recession-strain constant V_0:

$$G_0 = \frac{GH_0}{V_0}\,\mathrm{m^2\,s^{-2}\,kg^{-1}}\left(\mathrm{J/kg^2}\right). \tag{4}$$

Kepler's 3rd law based on LEP

Centripetal force F to be constant velocity circular motion the inertial mass m_i is

$$F = m_i r\omega^2 = m_i v^2/r. \tag{5}$$

By the active gravitational mass M_a and passive gravitational mass m_p, universal gravitation is

$$F = GM_a m_p/r^2. \tag{6}$$

By using Equations (5) and (6), the equilibrium of forces is:

$$m_i v^2/r = GM_a m_p/r^2. \tag{7}$$

By using Equations (7) and using the equivalence principle of light's momentum (LEP) $\gamma = c/w = m_i/m_p$, the equilibrium of potential energies is:

$$m_i v^2 = G(M_a m_i/\gamma)/r. \tag{8}$$

By using Equations (5) and (8), the equilibrium of potentials is:

$$v^2 = \omega^2 r^2 = G(M_a/\gamma)/r. \tag{9}$$

By using Equations (2) and (9), the equilibrium of potentials in consideration of the recession stretch Λ is:

$$v^2 = \omega^2 r^2 = \Lambda G(M_a/\gamma)/r. \tag{10}$$

By using Equations (3) and (10) and using $\omega = 2\pi/T$, Kepler's 3rd law $r^3 = aT^2$ based on LEP is

$$\begin{aligned} r^3 &= \frac{\Lambda G(M_a/\gamma)}{\omega^2} = \frac{\Lambda G(M_a/\gamma)}{4\pi^2}T^2 \\ r^2 &= \frac{G_x(M_a/\gamma)}{4\pi^2}T^2 \\ r &= \frac{\sqrt{G_x(M_a/\gamma)}}{2\pi}T = \frac{v}{\omega}. \end{aligned} \tag{11}$$

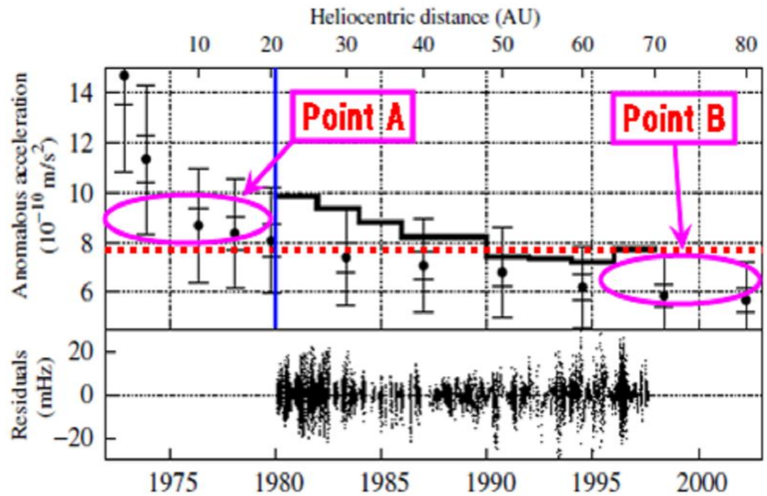

Figure 1. [The red dotted line is 7.84 ± 0.01 × 10−10 m/s² (Turyshev and Toth, 2010), and the pink circle is Discussion Point A, B.] to [Figure 3 (Turyshev et al., 2012): Comparison of the thermally-induced and anomalous accelerations for Pioneer 10. The estimated thermal acceleration is shown with error bars. The stochastic acceleration estimate from (Turyshev et al., 2011) appears as a step function].

RESULTS AND DISCUSSION

Pioneer anomaly

Data for short distances (that is, less than 20 au from the Sun) is restored to the original state and is analysed. One report suggests that the anomaly is caused by thermal radiation (Turyshev et al., 2012).discussion to a base in Figure 1 about it include: Discussion Point A, it thus becomes difficult to explain the Pioneer anomaly by modified gravitation theories, such as MOND or MOG, where gravity or the gravitational constant changes as a function of distance. Discussion Point B, the P10 data at the furthest distance flattened and increased (but within experimental uncertainty) which is inconsistent with a declining thermal cause (Hodge, 2013; Boom, 2013). Discussion Point Other, in addition, it is difficult to envision a solar neighbourhood that does not have dark matter (Bidin et al., 2012) to explain the Pioneer anomaly by the dark-matter hypothesis. As for the major cause of the slowdown, there is no conclusive evidence that the emission of the heat is the cause of the slowdown, nor for other arguments such as the effect of expanding space on photons (Kopeikin, 2012). It is strange that there is no gravity anomaly in the heliosphere, although we have an inexplicable problem, such as the galactic rotation curve, which is based only on the matter that is visible. Furthermore, there is the discussion that insisted on "If the Pioneer anomaly has a gravitational origin, it would, according to the equivalence principle, distort the motions of the planets in the Solar System" Tangen, 2007). However it is an inherent problem of the general relativity based on Weak equivalence principle (WEP) and Einstein's equivalence principle (EEP) "After an illustration by comparing the status of time in Einsteinian physics with that of the vertical direction in Newtonian physics, it was concluded that there is no pertinent notion of time in Einsteinian theories." (Lachieze, 2014, 2007; Mizony and Lachieze, 2005). This paper proposes that the Doppler blueshift that revealed the reduction in Pioneer's speed relative to the Sun is due to flat gravity that is caused by cosmic expansion. The decrease Δv in the velocity of the receiver relative to the source with blueshift Δf (5.99 ± 0.01 × 10^{-9} Hz) for frequency f_0 (2.29 GHz) is:

$$\Delta v = \Delta f \frac{c}{f_0} \cong 7.84 \times 10^{-10} \,\mathrm{m/s}, \quad (12)$$

which is within the error of (7.84 ± 0.01 × 10^{-8} cm/s²) from our formal solution for the Pioneer anomaly that was obtained from the available data (Turyshev and Toth, 2010). The slowdown (escape speed) of Pioneer that is due to flat gravity is calculated from the decrease in wave speed by using Equations (1) and (10) and using the expression $c^2 = w^2 + 2G_x M$ where c is the speed of light in vacuum and the wave speed in a gravitational field is:

$$2eG(M_s/\gamma)/r = 2G_0(M_s/\gamma) = c^2 - w^2$$
$$= c^2 - (c - \Delta v)^2 = 2c\Delta v - \Delta v^2 \approx 2c\Delta v. \quad (13)$$

By using Equations (4), (13) and using a solar mass M_s = 1.989 × 10^{30} kg (Astrodynamic Constants), the specific potential constant is:

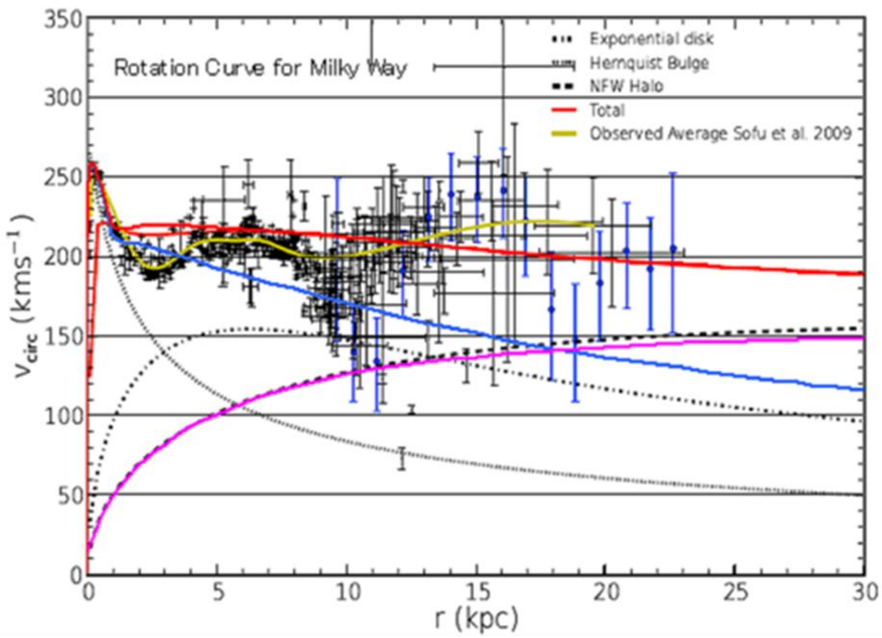

Figure 2. Adjusted the rotation curve (red) by Total gravity to Figure 10 (Kafle et al., 2012), and the rotation curve (blue) by Newtonian gravity and the rotation curve (pink) by Flat gravity were added.

$$G_0 = \frac{GH_0}{V_0} \approx \frac{c\Delta v}{(M_s/\gamma)} \cong 1.18\times10^{-31}\ \text{J/kg}^2. \quad (14)$$

In Equation (14), the specific potential constant G_0 is the gravitational mass and a proportionality constant for the blueshift. Transforming Equation (14) gives the recession strain constant V_0:

$$V_0 = \frac{GH_0}{G_0} \cong 1{,}240\ \text{m/s}. \quad (15)$$

The ratio of solar mass to total gravitational mass $M_0 = c^3/(2GH_0)$ of the observable universe (Kragh, 1999) is:

$$\frac{M_0}{(M_s/\gamma)} = \frac{c^2}{2V_0\Delta v} \cong 4.62\times10^{22}. \quad (16)$$

In addition, the specific potential constant G_0 is a proportionality constant of flat gravity: $G_0M = Mc^3/(2M_0V_0)$. It acts on gravitational mass and gives the total observable gravitational mass of the universe.

Galaxy rotation problem

From Newton's theory, the galactic rotational speed is:

$$v_r = \sqrt{G(M_g/\gamma)/r}\ \text{m/s}. \quad (17)$$

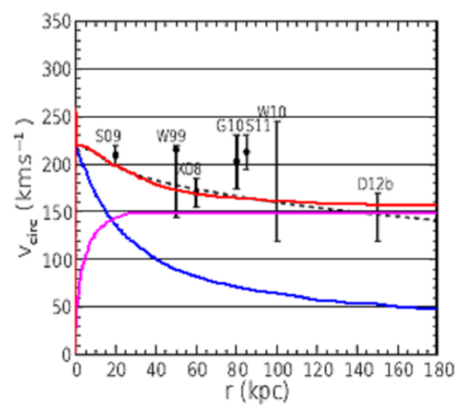

Figure 3. Widened Figure 11 (Kafle et al., 2012) by the setting that gravitational mass *Mg* (approximately 100 billion times of Solar mass) of the Milky Way galaxy did not increase from 30kpc to 180kpc.

In terms of the specific potential G_x, this is:

$$v_t = \sqrt{G_x(M_g/\gamma)} = \sqrt{(G/r + G_0)(M_g/\gamma)}\ \text{m/s}. \quad (18)$$

Therefore, given the galactic rotational speed V_t and the radius r, we can determine the galactic gravitational mass M_g. this calculation was applied to Figure 2 and 3 of the STELLAR HALO model of the Milky Way galaxy (Kafle et al., 2012) [the Milky Way has an inner and outer halo that

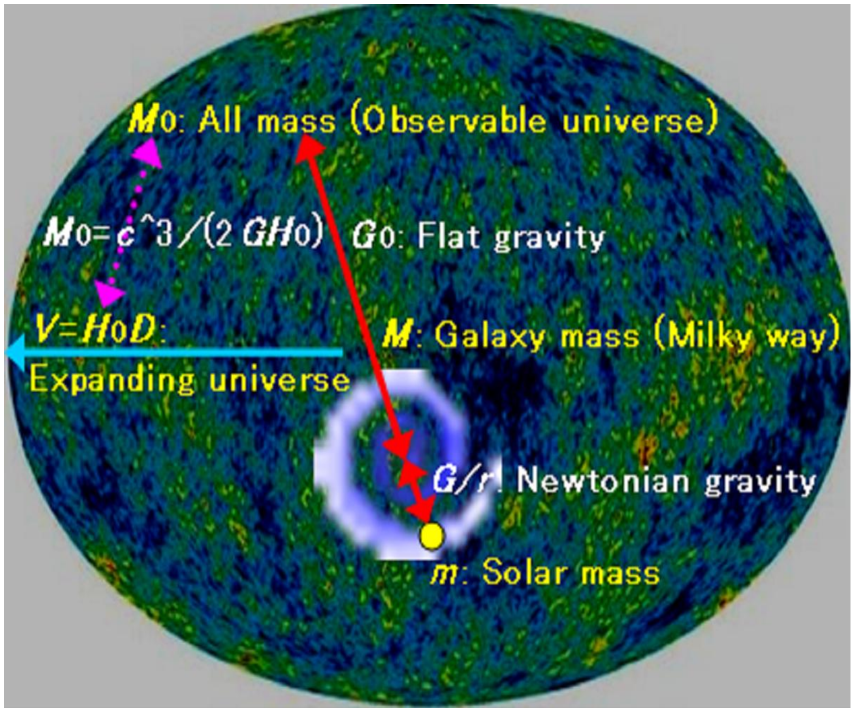

Figure 4. Theory of flat gravity that is based on Hubble's law of an expanding universe and newtonian gravitation.

spreads far and wide. It is in the latter that flat gravity flattens the velocity distribution curve]. The curve for dark matter (that is, Halo) and the flat gravity curve are similar, except that a discrepancy emerges for large *r* (kpc). However, examples such as Abell 520 are observed and indicate that dark matter exists far from the galactic disk and bulge (Mahdavi et al., 2007). Such examples cannot be explained by the conventional dark-matter hypothesis. Because flat gravity extends to an infinite distance, if flat gravity exists, it is indifferent to dark matter (Figure 4).

Small-scale crisis

The lambda Cold Dark Matter (Λ-CDM) model which added the effect (cosmic constant Λ) of the accelerating expansion of the universe to dark matter = Cold Dark Matter (CDM) which can disregard collisionless damping is a standard model of structure formation. However, as for the Λ-CDM model, disagreement with observation is pointed out in the small scale (below a Galaxy scale) (D'Onghia and Lake, 2004). Missing satellite problem (Klypin et al., 1999; Moore et al., 1999): Near the Milky Way galaxy (local group of galaxies), tens of dwarf galaxies (satellite galaxy) exist. However, N-body simulation of a Λ-CDM model is predicting that dark matter halo of about 500 dwarf galaxy mass exists in the same range. This suggests a possibility that the CDM model is wrong. Cuspy halo problem (Blok, 2009): According to the N-body simulation, a center becomes high-density by the very cusp of the density profile of dark matter halo. However, if it asks for a density profile from observation of the rotation curve of a dwarf galaxy, the profile of such a cusp will not be found. There are two huge black-holes in the bulge of the Andromeda Galaxy, and the material density of the central part is not high (Corbelli et al., 2010). Flat gravity and a dark matter curve are in agreement if r (kpc) becomes large (Figure 5). Moreover, the central part does not become high-density like the density profile of CDM. Those problems seem to adjust forcibly by the dark matter hypothesis.

Large-scale crisis

The scale of Hercules-Corona Borealis Great Wall is very huge. At the maximum of the size presumed from distribution of the gamma-ray burst, length is 10 billion light years and width is 7,200 million light years (Horvath et al., 2013). In the CDM model, the shock wave which occurred in the universe after the Big-Bang is assumed to be the base which makes the large-scale structure of the present universe. The size of the large-scale structure which arises from it should not exceed about 1,200 million light years (Yadav et al., 2010). This may show that it is unsuitable to predict the homogeneity of the actual universe and formation of large-scale structure by the CDM hypothesis. The Table 1 is the table which summarized the above.

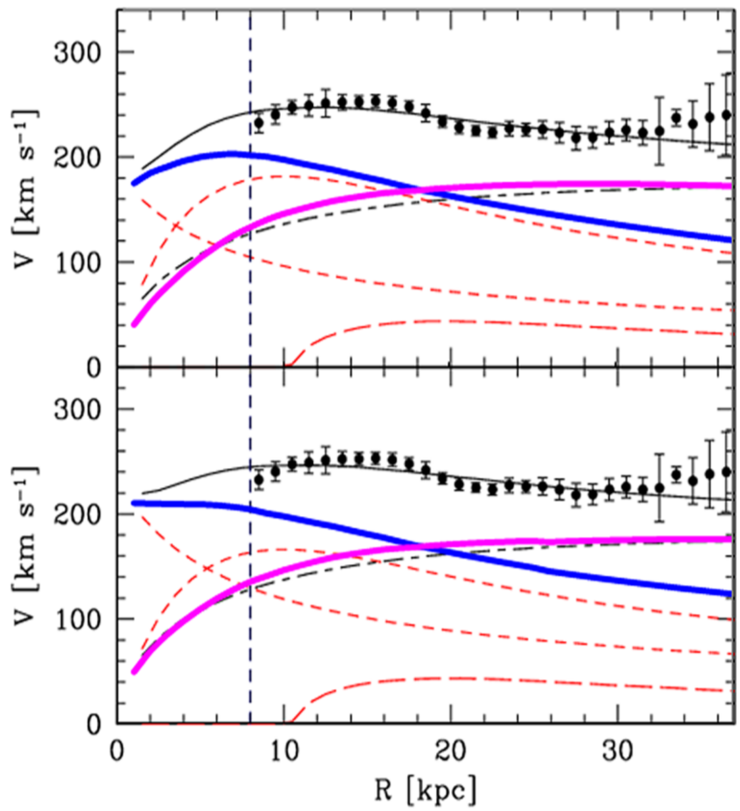

Figure 5. Adjusted the rotation curve (blue) by Newtonian gravity and the rotation curve (pink) by Flat gravity to Figure 14 (Corbelli et al., 2010). The M31 rotation curve (points) and the best fitting mass model (solid line) using the NFW dark halo profile with C = 12 in the frame of CDM. Also shown are the dark halo contribution (dot dashed line), the stellar disk and bulge (short dashed line) and the gas contribution (long dashed line). The bottom panel refers to the case ((M/L)d = (M/L)b = 4.2M /L). The top panel refers to the best fit when the mass-to-light ratio of the disk and the bulge are two independent variables. For the best fit (M/L)d = 5.0 and an (M/L)b = 2.7 M /L.

Table 1. Summary of this paper.

Open problem	Microscopic	Pioneer anomaly	Galaxy rotation	Over galaxy
MOND	Unknown	Unknown	Explanation	Unknown
MOG	Unknown	Unknown	Explanation	Unknown
Dark Matter	Unknown	Unknown	Explanation	Unknown
Flat Gravity	Unknown	Explanation	Explanation	Unknown

Conclusion

The specific potential constant that was calculated from the abnormal acceleration of the planetary probe pioneer with respect to the Sun is $G_0 = 1.18\times10^{-31}$ J/kg^2. Given a galactic mass approximately 100 billion times that of the Sun gives a galactic rotational speed of $v_g = (G_0M_g/\gamma)^{1/2}$ = 150 km/s. The gravitational potential is $-GM(1/r)$ in a static universe; however, the influence of cosmic expansion should be considered in an expanding universe by using $-GM(1/r)(1 + \text{expansion}) = -(G/r + G_0)M$ for all scales from the microscopic to the large scale of the universe. This resembles the relation between the longitudinal Doppler effect $(1 - v/c)$ and the transverse

Doppler effect $(1 - v^2/c^2)^{1/2}$. Flat gravity can be named longitudinal gravity if Newtonian gravity is named transverse gravity. None of the theories (flat gravity, dark matter or modified gravitation) can explain all scales. However, flat gravity offers the possibility to explain small scales, such as the microscopic scale, which may increase correction term in the Newtonian gravitational potential, and the large scale, such as the intergalactic scale. It is important to gain experience with various scales for the expanding universe because we are familiar with Kepler's laws and Newtonian mechanics but need more experience with flat gravity. Not only an apple but all the matter in the expanding universe are in the state of free-fall.

Conflict of Interest

The author has not declared any conflict of interest.

ACKNOWLEDGEMENTS

The author thank the late Dr. Hubble who discovered the expanding universe and Professor Nyanpan who taught him gravity.

REFERENCES

Ade PAR, Aghanim N, Alves MIR, Armitage-Caplan C, Arnaud M, Ashdown M, Atrio-Barandela F, Aumont J, Aussel H, Baccigalupi C, Banday AJ, Barreiro RB, Barrena R, Bartelmann M, Bartlett JG, Bartolo N, Basak S, Battaner E, Battye R, Benabed K, Benoît A, Benoit-Lévy A, Bernard JP, Bersanelli M, Bertincourt B, Bethermin M, Bielewicz P, Bikmaev I, Blanchard A, Bobin J, Bock JJ, Böhringer H, Bonaldi A, Bonavera L, Bond JR, Borrill J, Bouchet FR, Boulanger F, Bourdin H, Bowyer JW, Bridges M, Brown ML, Bucher M, Burenin R, Burigana C, Butler RC, Calabrese E, Cappellini B, Cardoso JF, Carr R, Carvalho P, Casale M, Castex G, Catalano A, Challinor A, Chamballu A, Chary RR, Chen X, Chiang HC, Chiang LY; Chon G, Christensen PR, Churazov E, Church S, Clemens M, Clements DL, Colombi S, Colombo LPL, Combet C, Comis B, Couchot F, Coulais A, Crill BP, Cruz M, Curto A, Cuttaia F, Da Silva A, Dahle H, Danese L, Davies RD, Davis RJ, Bernardis PD, Rosa AD, Zotti GD, Déchelette T, Delabrouille J, Delouis JM, Démoclès J, Désert FX, Dick J, Dickinson C, Diego JM, Dolag K, Dole H, Donzelli S, Doré O, Douspis M, Ducout A, Dunkley J, Dupac X, Efstathiou G, Elsner F, Enßlin TA, Eriksen HK, Fabre O, Falgarone E, Falvella MC, Fantaye Y, Fergusson J, Filliard C, Finelli F, Flores-Cacho I, Foley S, Forni O, Fosalba P, Frailis M, Fraisse AA, Franceschi E, Freschi M, Fromenteau S Frommert M, Gaier TC, Galeotta S, Gallegos J, Galli S, Gandolfo B, Ganga K, Gauthier C, Génova-Santos RT, Ghosh T, Giard M, Giardino G, Gilfanov M, Girard D, Giraud-Héraud Y, Gjerløw E, González-Nuevo J, Górski KM, Gratton S, Gregorio A, Gruppuso A, Gudmundsson JE, Haissinski J, Hamann J, Hansen FK, Hansen M, Hanson D, Harrison DL, Heavens A, Helou G, Hempel A, Henrot-Versillé S, Hernández-Monteagudo C, Herranz D, Hildebrandt SR, Hivon E, Ho S, Hobson M, Holmes WA, Hornstrup A, Hou Z, Hovest W, Huey G, Huffenberger KM, Hurier G, Ilić S, Jaffe AH, Jaffe TR, Jasche J, Jewell J, Jones WC, Juvela M, Kalberla P, Kangaslahti P, Keihänen E, Kerp J, Keskitalo R, Khamitov I, Kiiveri K, Kim J, Kisner TS, Kneissl R, Knoche J, Knox L, Kunz M, Kurki-Suonio H, Lacasa F, Lagache G, Lähteenmäki A, Lamarre JM, Langer M, Lasenby A, Lattanzi M, Laureijs RJ, Lavabre A, Lawrence CR, Le Jeune M, Leach S, Leahy JP, Leonardi R, León-Tavares J, Leroy C, Lesgourgues J, Lewis A, Li C, Liddle A, Liguori M, Lilje PB, Linden-Vørnle M, Lindholm V, López-Caniego M, Lowe S, Lubin PM, Macías-Pérez JF, MacTavish CJ, Maffei B, Maggio G, Maino D, Mandolesi N, Mangilli A, Marcos-Caballero A, Marinucci D, Maris M, Marleau F, Marshall DJ, Martin PG, Martínez-González E, Masi S, Massardi M, Matarrese S, Matsumura T, Matthai F, Maurin L, Mazzotta P, McDonald A, McEwen JD, McGehee P, Mei S, Meinhold PR, Melchiorri A, Melin JB, Mendes L, Menegoni E, Mennella A, Migliaccio M, Mikkelsen K, Millea M, Miniscalco R, Mitra S, Miville-Deschênes MA, Molinari D, Moneti A, Montier L, Morgante G, Morisset N, Mortlock D, Moss A, Munshi D, Murphy JA, Naselsky P, Nati F, Natoli P, Negrello M, Nesvadba NPH, Netterfield CB, Nørgaard-Nielsen HU, North C, Noviello F, Novikov D, Novikov I, O'Dwyer IJ, Orieux F, Osborne S, O'Sullivan C, Oxborrow CA, Paci F, Pagano L, Pajot F, Paladini R, Pandolfi S, Paoletti D, Partridge B, Pasian F, Patanchon G, Paykari P, Pearson D, Pearson TJ, Peel M, Peiris HV, Perdereau O, Perotto L, Perrotta F, Pettorino V, Piacentini F, Piat M, Pierpaoli E, Pietrobon D, Plaszczynski S, Platania P, Pogosyan D, Pointecouteau E, Polenta G, Ponthieu N, Popa L, Poutanen T, Pratt GW, Prézeau G, Prunet S, Puget JL, Pullen AR, Rachen JP, Racine B, Rahlin A, Räth C, Reach WT, Rebolo R, Reinecke M, Remazeilles M, Renault C, Renzi A, Riazuelo A, Ricciardi S, Riller T, Ringeval C, Ristorcelli I, Robbers G, Rocha G, Roman M, Rosset C, Rossetti M, Roudier G, Rowan-Robinson M, Rubiño-Martín JA, Ruiz-Granados B, Rusholme B, Salerno E, Sandri M, Sanselme L, Santos D, Savelainen M, Savini G, Schaefer BM, Schiavon F, Scott D, Seiffert MD, Serra P, Shellard EPS, Smith K, Smoot GF, Souradeep T, Spencer LD, Starck JL, Stolyarov V, Stompor R, Sudiwala R, Sunyaev R, Sureau F, Sutter P, Sutton D, Suur-Uski AS, Sygnet JF, Tauber JA, Tavagnacco D, Taylor D, Terenzi L, Texier D, Toffolatti L, Tomasi M, Torre JP, Tristram M, Tucci M, Tuovinen J, Türler M, Tuttlebee M, Umana G, Valenziano L, Valiviita J, Van Tent B, Varis J, Vibert L, Viel M, Vielva P, Villa F, Vittorio N, Wade LA, Wandelt BD, Watson C, Watson R, Wehus IK, Welikala N, Weller J, White M, White SDM, Wilkinson A, Winkel B, Xia JQ, Yvon D, Zacchei A, Zibin JP, Zonca A (2013). Planck 2013 results. I. Overview of products and scientific results. preprint arXiv: 1303.5062.

Anderson JD, Laing PA, Lau EL, Liu AS, Nieto MM, Turyshev, SG (1998). Indication, from Pioneer 10/11, Galileo, and Ulysses data, of an apparent anomalous, weak, long-range acceleration. Phys. Rev. Lett. 81(14):2858. http://dx.doi.org/10.1103/PhysRevLett.81.2858

Astrodynamic Constants, http://ssd.jpl.nasa.gov/?constants, Accessed 7 July 2014.

Bidin CM, Carraro G, Méndez RA, Smith R (2012). Kinematical and chemical vertical structure of the galactic thick disk. II. A lack of dark matter in the solar neighborhood. Astrophys. J. 751(1):30. http://dx.doi.org/10.1088/0004-637X/751/1/30

Blok WJGD (2009). The core-cusp problem. Advances in Astronomy. 2010.

Boom PGT (2013). The Pioneer Anomaly: An inconvenient reality or NASA's 12 year misconception?. preprint arXiv: 1307.0537.

Brownstein JR, Moffat JW (2006). Galaxy rotation curves without nonbaryonic dark matter. Astrophys. J. 636(2): 721. http://dx.doi.org/10.1086/498208

Corbelli E, Lorenzoni S, Walterbos R, Braun R, Thilker D (2010). A wide-field HI mosaic of Messier 31: II. The disk warp, rotation, and the dark matter halo. Astron Astrophys. 511.

D'Onghia E, Lake G (2004). Cold dark matter's small-scale crisis grows up. Astrophys. J. 612(2):628. http://dx.doi.org/10.1086/422794

Hodge JC (2013). Comments on The Pioneer Anomaly: an inconvenient reality or NASA's 12 year misconception. L4C 3N0 Canada E-mail Web Site Series. 1.

Horvath I, Hakkila J, Bagoly Z (2013). The largest structure of the Universe, defined by Gamma-Ray Bursts. *arXiv* preprint arXiv:1311.1104.

Hubble E (1929). A relation between distance and radial velocity among extra-galactic nebulae. Proc. Natl. Acad. Sci. U.S.A. 15(3):168-173. http://dx.doi.org/10.1073/pnas.15.3.168

Kafle PR, Sharma S, Lewis GF, Bland-Hawthorn J (2012). Kinematics of the Stellar Halo and the Mass Distribution of the Milky Way Using Blue Horizontal Branch Stars. Astrophys. J. 761(2):98. http://dx.doi.org/10.1088/0004-637X/761/2/98

Klypin A, Kravtsov AV, Valenzuela O, Prada F (1999). Where are the missing galactic satellites?. Astrophys. J. 522(1): 82. http://dx.doi.org/10.1086/307643
Kopeikin SM (2012). Celestial ephemerides in an expanding universe. Phys. Rev. D. 86(6):064004. http://dx.doi.org/10.1103/PhysRevD.86.064004
Kragh H (1999). Cosmology and controversy: The historical development of two theories of the universe. Princeton University Press: 212.
Lachieze-Rey M (2007). Cosmology in the solar system: The Pioneer effect is not cosmological. Class. Quantum Grav. 24(10):2735. http://dx.doi.org/10.1088/0264-9381/24/10/016
Lachieze-Rey M (2014). In search of relativistic time. Stud. Hist. Philos. M. P. 46: 38-47. http://dx.doi.org/10.1016/j.shpsb.2014.01.001
Mahdavi A, Hoekstra H, Babul A, Balam DD, Capak PL (2007). A dark core in Abell 520. Astrophys. J. 668(2):806. http://dx.doi.org/10.1086/521383
Milgrom M (1983). A modification of the Newtonian dynamics as a possible alternative to the hidden mass hypothesis. Astrophys. J. 270: 365-370. http://dx.doi.org/10.1086/161130
Mizony M, Lachieze-Rey M (2005). Cosmological effects in the local static frame. A&A 434: 45-52.
Moore B, Ghigna S, Governato F, Lake G, Quinn T, Stadel J, Tozzi P (1999). Dark matter substructure within galactic halos. Astrophys. J. Lett. 524(1): L19. http://dx.doi.org/10.1086/312287
Rubin VC, Ford Jr WK, Thonnard N (1980). Rotational properties of 21 SC galaxies with a large range of luminosities and radii, from NGC 4605/R= 4kpc/to UGC 2885/R= 122 kpc. Astrophys. J. 238: 471-487. http://dx.doi.org/10.1086/158003
Tangen K (2007). Could the Pioneer anomaly have a gravitational origin?. Phys. Rev. D. 76(4): 042005. http://dx.doi.org/10.1103/PhysRevD.76.042005
Turyshev SG, Toth VT (2010). The pioneer anomaly. Living Rev. Relat. 13(4):9-175.
Turyshev SG, Toth VT, Kinsella G, Lee SC, Lok SM, Ellis J (2012). Support for the thermal origin of the Pioneer anomaly. Phys. Rev. Lett. 108(24):241101. http://dx.doi.org/10.1103/PhysRevLett.108.241101
Yadav JK, Bagla JS, Khandai N (2010). Fractal dimension as a measure of the scale of homogeneity. Mon. Not. R. Astron. Soc. 405(3):2009-2015.
Zwicky F (1933). Die rotverschiebung von extragalaktischen nebeln. Helv. Phys. Acta. 6:110-127.
Zwicky F (1937). On the Masses of Nebulae and of Clusters of Nebulae. Astrophys. J. 86: 217. http://dx.doi.org/10.1086/143864

academicJournals

Vol. 9(22), pp. 495-505, 30 November, 2014
DOI: 10.5897/IJPS2014.4192
Article Number:840377B48840
ISSN 1992 - 1950

http://www.academicjournals.org/IJPS

International Journal of Physical Sciences

Full Length Research Paper

Measurement, prediction and modeling the impact of vibration as the possibility of protection cultural heritage objects

Sebastian Toplak, Andrej Ivanic, Primoz Jelusic and Samo Lubej*

Faculty of Civil Engineering, University of Maribor, Smetanova 17, 2000 Maribor, Slovenia.

Received 26 July, 2014; Accepted 5 November, 2014

This article describes the possibility of using prognostic equations and the theory of fuzzy logic to predict the intensity of vibrations resulting from the use of construction machinery and heavy traffic. Vibrations from construction machinery can be particularly dangerous if they affect heritage buildings. By analyzing the measured results of vibrations at various facilities, we found that using the theory of fuzzy logic and appropriate modeling we can well predict the intensity of vibration caused by heavy traffic and vibration compaction with vibratory rollers.

Key words: Fuzzy logic, ground vibrations, vibrations monitoring, vibrations prognosis, neural networks.

INTRODUCTION

Experts in sustainable planning of roads are facing the problem of how to prepare their proposals for the authorities so that they will be able to support their decisions with numbered facts. A typical example of such a problem is erecting traffic infrastructure in locations where only part of factors can be shown quantitatively and costs estimated accordingly (mainly construction and maintenance costs). Contrary to this, we tend to show numerous consequences, both costs and benefits, qualitatively, which means descriptively, or we completely ignore the obvious consequences of an intervention in space which may cause social harm or benefits, damage to cultural heritage buildings or create the need of displacement. We are not able to adequately quantify costs and benefits not estimate costs. Another problem of sustainable road design is a deficient judgment of benefits and consequences of road's total life cycle from "ideas" and "construction" to "preservation" and "degradation".

In this paper we focused on and analyzed two very common phenomena occurring during the construction and operation of roads and ancillary facilities: vibrations arising from construction machinery and vibrations arising from freight traffic. The vast majority of construction machinery used in earthworks produces harmful vibrations. Many earthworks, such as piling and vibratory compaction of materials cause vibrations that can be transmitted in soil to nearby facilities. Because of vibrations, generated dynamic forces can cause damage to nearby structures. Old buildings are the most vulnerable of all structures.

An adaptive network fuzzy inference system (ANFIS) is used for predicting the intensity of vibration. ANFIS is considered to be one of the intelligent tools to understand

*Corresponding author. E-mail: samo.lubej@guest.arnes.si

the complex problems (Jang, 1993). Therefore, ANFIS is being successfully used in many industrial areas as well as in research (Faravelli and Yao, 1996; Provenzano et al., 2004; Gokceoglu et al., 2004; Rangel et al., 2005; Kayadelen et al., 2009). Khandelwal (2012) predict the blast induced ground vibration using different conventional vibrations predictors and artificial neural network (ANN) at a surface of coal mine and it was found out that the ANN model based on multiple input parameters have better prediction capability than conventional vibration predictors.

PHYSICAL CHARACTERISTICS OF CONSTRUCTION MACHINERY AND FREIGHT TRAFFIC

Slovenia has no standards of its own in the field of vibration measurements. By joining the European Union, we could take over the well established European standards in this field, such as DIN 4150, Swiss Standard SN 640 312a, British Standard (BS) 7385 and BS 6472. In Europe the standard DIN 4150 is most commonly used for measuring and assessing effects of vibrations on buildings. This standard prescribes the maximum ground vibration velocity which is 3 mm/s for heritage buildings, 5 mm/s for residential buildings and 10 mm/s for industrial facilities. The maximum ground vibration velocity is given with special curves depending on ground vibration frequency.

Many earthworks, such as driving pilots and sheet piling, vibratory compaction of earth materials as well as operation of heavy construction equipment, cause vibrations that can be transmitted to nearby buildings. Dynamic forces generated by these vibrations can cause damage to the buildings. When designing and planning activities at the site we need to assess possible effects of vibrations, and adjust work of vibratory machines so as to minimize their effects on the surrounding buildings (Achmus and Kaiser, 2006). The effects of vibrations caused by construction machinery may vary depending on numerous factors, such as the intensity of sources of vibration, different soil composition and its quality between the sources of vibration and the building, the quality of foundations, building dimensions and the quality of built-in materials. The effects of vibrations are enhanced by the intensity and duration of vibrations and by the frequency and number of vibration events. The effects of vibrations caused by construction machinery may interfere with users of a building and damage the building, since there is shaking and moving that can change structural integrity of the building to such an extent that its stability is at risk. In vibratory compaction of loose soil layers we dynamically compact upper soil layers. In these construction processes vibrations are transmitted through the soil to neighbouring buildings causing damage to them. When planning construction, possible impacts of vibrations should thus be assessed and resulting risks and building machines selected so that their impact on surrounding buildings is prevented or at least minimized.

Since 2002 the Slovene statistical office has been performing research about environmental costs arising from different environmental purposes in accordance with the European statistical classification of activities relating to the protection of the environment (CEPA). Data are being collected on investment in environmental protection, current expenses for the environment and income from environmental protection activities. CEPA is a general, multi-purpose and functional classification which is used for classifying the activities for environmental protection. According to this classification the protection against noise and vibrations is also recorded. This protection covers the reduction of noise and vibrations caused by road and rail transport, as well as air transport and shipping. According to the above criteria, activities are foreseen, such as monitoring, traffic management, and erection of sound barriers or anti-vibration devices (Statistical Office, 2009). Traffic vibrations are common concerns of society because they often cause problems to people and structures. They constitute an external source and result from heavy traffic such as buses and trucks. Passenger cars and light trucks rarely cause vibrations that are discernible in buildings. Road transport usually causes vibrations in the frequency range from 5 to 25 Hz and ground vibration from 0.05 to 25 mm/s (Hunaidi, 2000). The frequencies and the vibration velocity depend on numerous factors, such as pavement conditions (especially damage and roughness), the speed and weight of vehicles, a vehicle suspension system, the type of soil, the season, the distance between the road and the building and the type of the building.

MEASUREMENTS, DESCRIPTION OF THE EXPERIMENT AND THE RESULTS

Vibration measurements were performed separately for three types of vibrations. We have measured the impact of the vibrating roller on the residential and on heritage object, where motorway was under construction. The second segment of monitoring comprised the measuring of effects at the residential building, during driving and pulling of sheet piling when the round about and the access to a new motorway was under construction. In the third case we measured the impact of heavy traffic on the residential building.

Earthquake intensity, which results from operation of construction machines or traffic, can be measured with seismographs. Seismographs are portable devices that can be placed wherever it is necessary to measure the intensity of vibrations. They measure vibrations which are transmitted to the seismic mass of a geophone and then to three perpendicularly mounted electromagnetic coils.

Table 1. Technical characteristics of dynamic rollers.

Variables	HAMM 3520	AMMAN AC 110
Operating weight (kg)	12480	12100
Rear axle load (kg)	7320	7140
Vibration frequency (Hz)/amplitude (mm)	30/1,19	28-35/1,8-0,8

Vibration components induce voltage and hence electrical impulses in the winding. These impulses are transmitted to the electronic recording with a built-in microprocessor with a certain memory. Measurement values recorded in the memory can be processed analytically with the software. For vibration measurements, we used the measurement equipment of the manufacturer Instanel from Canada, namely the four-channel device Minimate Plus and the eight-channel device Minimate Plus with the associated linear microphone and the geophones. The impact of construction machinery, whose operation causes vibrations, and the impact of road freight transport are also measured by ground vibration velocity. Geophones can be used for these measurements as well as for assessing a building response to vibrations. Ground vibration velocity is usually measured at the source of vibration – on the ground in the immediate vicinity of a construction machine, on the ground in front of the foundation of the building observed, and at the foundation of the building. The results of measurements present the measured components of vibration velocity in all three orthogonal directions.

Effects of vibration from trucks

Heavy vehicle traffic was monitored in two cases during earthworks for the construction of the parking house. We measured vibrations on the gravel road caused by trucks with a total weight of 20 tons in the phase of driving off, and vibrations on the asphalt road caused by trucks with a total weight of 20 tons and running at a speed of 40 km/h.

Effects of vibration from a vibrating roller

The constructor of the motorway section used two types of construction machinery which causes vibrations. In compaction of road section the dynamic roller HAMM 3520 was used. The second dynamic roller was AMMAN AC 110. The following technical characteristics are presented in Table 1. We have measured the effects of vibrations during the operation of one vibrating roller and two synchronously operating rollers HAMM. The second measuring with vibrating roller AMMAN has ben measured the imapct of surface dynamic compaction, deep dynamic compaction and static compaction.The measuring instruments – Instantel Minimate Plus measuring station were activated manually, with a time interval between individual measurements of 10 s.

Effects of vibration from driving/pulling sheet pilling

The measurement of vibrations during the construction of new bridge in the old kernel of town was performed at 17 measuring points. Vibrations were measured at facilities, which are protected cultural heritage structures. The second part of measurements was performed on the residential building during the construction of a road roundabout. In both cases the sheet piling was used to protect the excavation or construction pit, respectively.

Prognosis of vibration

The prognosis of vibration based on vibration measurements, which were measured and the use of empirical equations by various authors. The use of prognostic equations as an option for reducing the negative effects of vibration.

Prognosis of vibration velocity from trucks

The measurements were analyzed with a model for predicting the intensity of vibration proposed by Watts (1990). The presented model is based on local degradation of the roadway surface, along which vehicles run with a certain speed, and the distance between the moving vehicle and the measuring point. The model is expressed as:

$$PPV = 0.028 \cdot a \cdot \left(v/48\right) \cdot t \cdot p \cdot \left(r/6\right)^{x}. \qquad (1)$$

Where: PPV = the peak particle velocity (mm/s), a = the maximum degradation of a surface or a defect (mm), v = the measured speed of a vehicle (km/h), t = the coefficient of soil supporting a roadway structure, p = the wheel index, which is over 0.75 for heavy vehicles when one wheel crosses a damaged spot, or 1 in other cases, r = the distance between the measuring point and the moving vehicle.

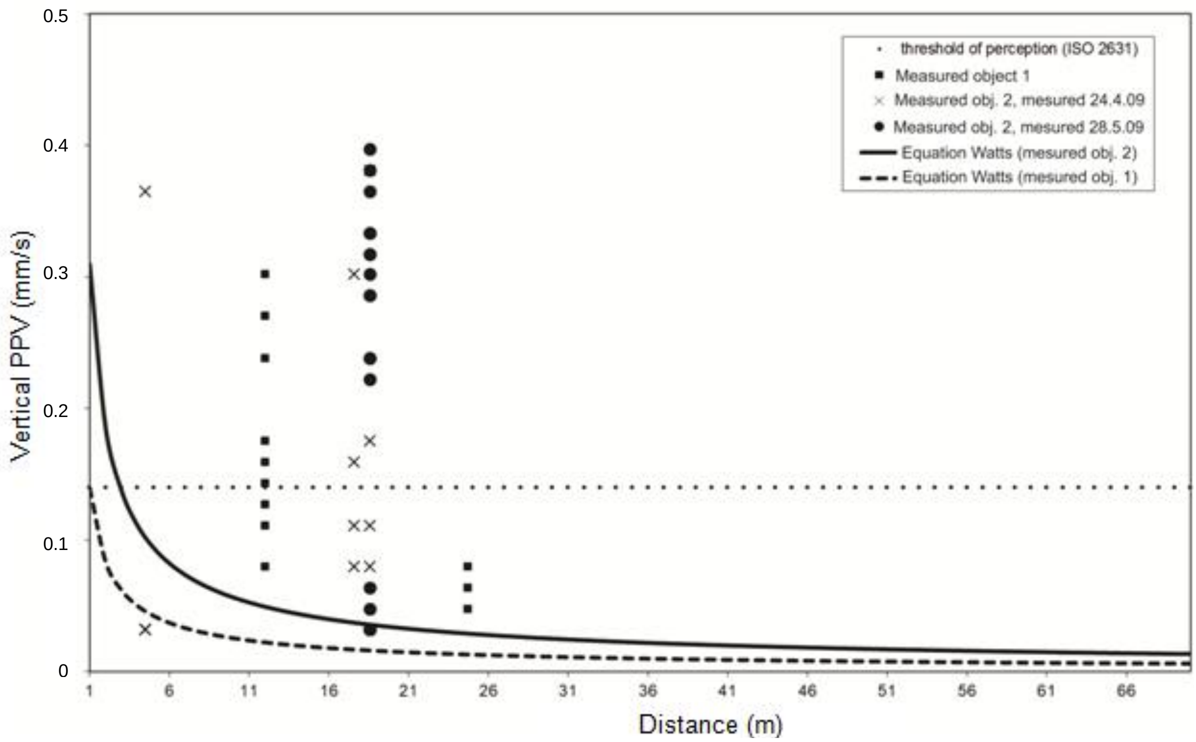

Figure 1. The results of the measured values using the prognostic equation for heavy trucks.

The value of the exponent x determines damping of vibrations and it depends on the site and the distance. The results of the effect of vibrations caused by heavy trucks are given in Figure 1.

Prognosis of vibration velocity from a a vibratory roller

To forecast the potential damage to structures, foundation oscillation velocity, not ground vibration velocity, is used as the base value. Maximum oscillation velocity changes at the transfer to foundations, mainly resulting in the reduction. In the case of resonance, there is a very slight, small increase in oscillation velocity. Due to unknown factors of the transfer of oscillations to the foundations of a building, it is useful to know direct equations to forecast maximal components of foundation oscillation velocity. This is practical because in measuring vibrations measuring devices are placed on foundations and not on the ground, which allows easy calibration of the equations. Such prognostic equations are mainly based on practical experience and are not yet widespread. Since vibratory energy of vibration machines is difficult to assess, a decisive parameter in these prognostic equations is the operating weight of the machine. To predict foundation oscillation velocity arising from vibration rolling we used two equations. The first Equation (2) is suggested by Philipps et al. (2010), and the second Equation (3) by Achmus et al. (2005).

$$v_{Fi,\max} = 1{,}1 \frac{\sqrt{G}}{r^{0,7}} \tag{2}$$

$$v_{Fi,\max} = K \frac{\sqrt{G}}{r} \tag{3}$$

Where: $v_{Fi,max}$ is the maximum foundation oscillation velocity (mm/s), G is the operating weight of the vibrating machine (t) and r is the distance from the vibration source to the foundation (m).

The coefficient K in Equation (2) is 4.31 for a 50% accuracy of results. We used the results of vertical and longitudinal components of foundation oscillation velocity, which are graphically presented in Figure 2, together with the lines of the prognostic Equations (2) and (3) and the relevant literature data (Achmus et al., 2005).

Prognosis of vibration velocity from driving/pulling sheet pilling

Ground and foundation vibration velocity is also taken as the basic physical quantity to predict the potential damage on buildings. In the transfer of vibrations from the ground to the foundations of the building the vibration velocity tends to decrease, yet it can increase in some

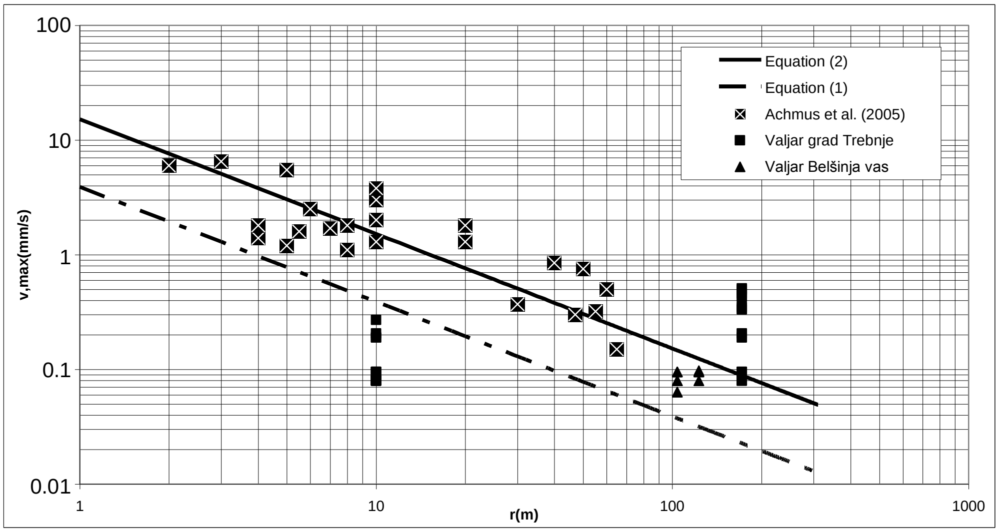

Figure 2. The measured versus predicted values of foundation oscillation velocity.

cases owing to resonance. Especially in pulling sheet piling, sudden changes can occur in vibration velocity in three orthogonal directions. Because of this it is very important to consider the highest measured value in forecasting and evaluating the effect of vibrations. In this case, we used the equation of Achmus et al. (2005), which reads:

$$v_{Fi,\max} = K_F \frac{\sqrt{\frac{W}{f}}}{r}. \tag{4}$$

Where: $\upsilon_{Fi,max}$ = the maximum foundation oscillation velocity (mm/s), W = the maximum power of the machine in watts, f = the operating frequency of the machine (s-1) and r = the distance from the source of vibration to the measuring point in (m).

The coefficient K_F is 7.9 for a 50% probability of increase, or 18.5 respectively for a 2.25% probability of increase. In analyzing the measured values given in Figure 3, we considered that in driving 7.1 kNm of energy is consumed, while in pulling 2.8 kNm. Vibration frequency is 28 Hz in both cases.

ANFIS MODEL FOR GROUND VIBRATION PREDICTION

The basic structure of the fuzzy inference system (FIS) was introduced by Zadeh (1965). In this type of FIS it is essentially to predetermine the rule structure and the membership functions. Human determined membership functions are subjective and differentiate from person to person. The standard methods, which transform human knowledge or experience into the fuzzy rules and membership functions, do not exist. Usually there is the collection of input/output data, which we would like to use for constructing the FIS model. The effective method for tuning the membership functions and to minimize the output error measure is the Adaptive-Network-Based Fuzzy Inference System (ANFIS). ANFIS (Jang, 1993) uses a given input/output data to construct a FIS, whose membership function parameters are tuned (adjusted) using either a back propagation algorithm alone or in combination with a least squares type of method. This adjustment allows fuzzy systems to learn from the data they are modelling. ANFIS only supports Sugeno-Takagi-Kang (1985) identification models, which should have only one output parameter. Adaptive network is a superset of all kinds of feed-forward neural networks with supervised learning capability (Rumelhart, 1986). ANFIS is a fuzzy inference system implemented in the framework of adaptive networks and uses the advantages of neural networks and fuzzy logic.

One of the most important stages in the ANFIS technique is data collection. The data was divided into training and checking datasets. Training datasets contains measurements of the vibration caused by trucks and vibratory roller. As an interface for mathematical modelling and data inputs/outputs the MATLAB (2010), a high-level technical computing language, was used.

Vibration caused by trucks

In this case, data is collected using noisy measurements, and the training data cannot be representative of all the features of the data that will be presented to the model. In this model, 15 measurements were used to build a model. Among which, 11 evaluations (70%) were used

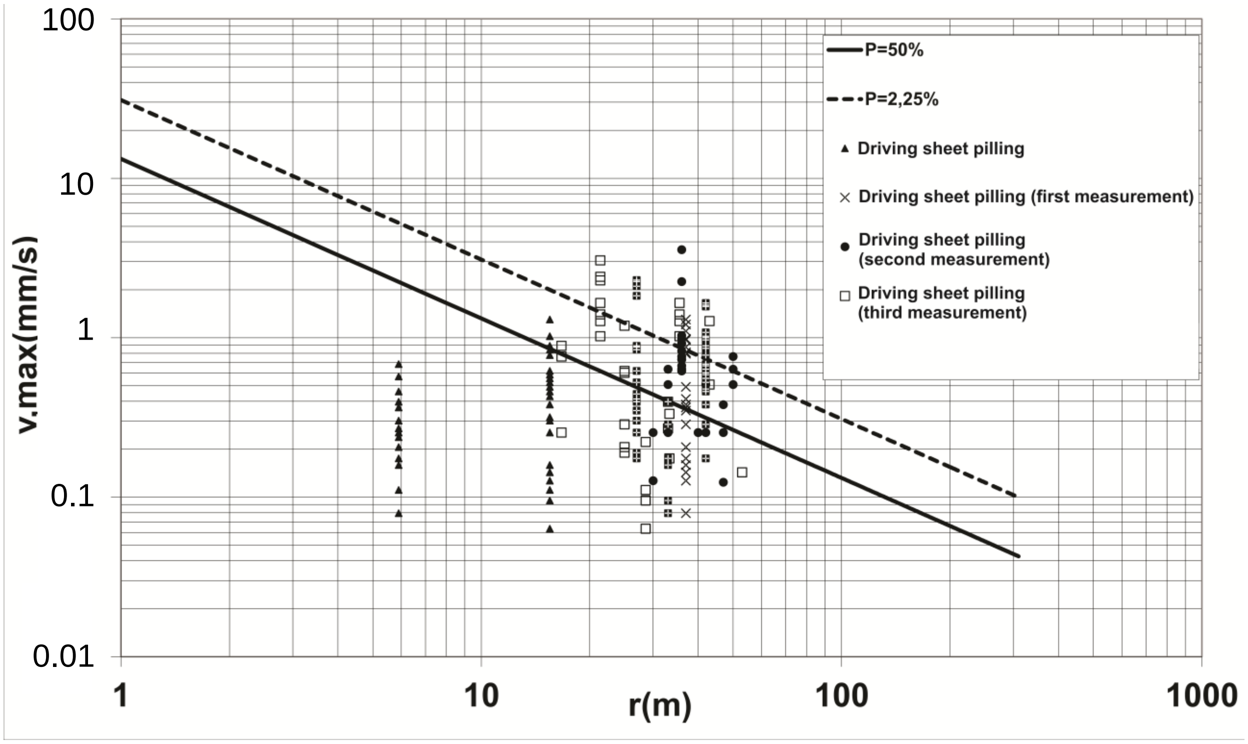

Figure 3. The measured values using the prognostic equation for driving/pulling sheet piling.

Table 2. Training data.

No. measurements	V (km/h)	r (m)	PPV (mm/s)
1	86	7	1.02
2	86	67	0.087
3	71	7	0.766
4	71	67	0.087
5	69	7	0.658
6	69	67	0.092
7	68	67	0.096
8	67	67	0.010
9	65	7	0.809
10	65	67	0.125
11	57	7	0.457

for the training of the ANFIS model, whereas 4 data sets (30%) were chosen for checking the model. Table 2 represents training data and Table 3 represents checking data.

PPV is predicted using ANFIS model based on two parameters (speed of a vehicle and the distance between the measuring point and the moving vehicle). The maximum degradation of a surface is 0.5 mm and the coefficient of soil supporting a roadway structure is 0.1. On the basis of the measured data we build model to predict PPV value for any speed of a vehicle and the distance between the measuring point and the moving vehicle (Figure 4).

ANFIS use a given input/output data to constructs a FIS whose membership function parameters are tuned (adjusted) using either a back propagation algorithm alone or in combination with a least squares type of method. This adjustment allows a fuzzy systems to learn from the data they are modeling. The hybrid algorithm is described in detail (Jang, 1993). The hybrid algorithm can reduce the error between FIS model and the data that we used to build and verify the model. The aim of ANFIS

Table 3. Checking data.

No. of measurements	V (km/h)	r (m)	PPV (mm/s)
1	70	7	0.502
2	70	67	0.094
3	67	7	0.851
4	67	67	0.103

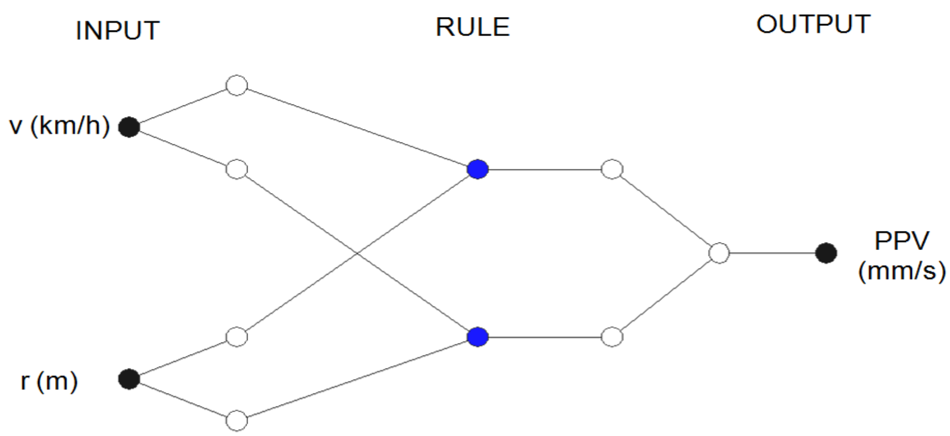

Figure 4. Suggested ANFIS for prediction of ground vibration caused by trucks.

Table 4. The ANFIS structure.

No. of training data sets	11
No. of checking data sets	4
Type	sugeno
No. of input membership functions	2
No. of output membership functions	2
No. of rules	2
And method	prod
Or method	probor
Defuzzification method	wtaver
Implication method	prod
Aggregation method	max

method is to minimize the root mean square error (RMSE) of the model to given attributes. Optimal parameters of the model were achieved when the RMSE is no longer decreasing. ANFIS structure for ground vibration prediction is summarized in Table 4.

Results of ANFIS model - vibration caused by trucks

Results of ANFIS model are shown in Figure 5. Surface shows the influence of speed of a vehicle and the distance between the measuring point and the moving vehicle on the peak particle velocity. ANFIS method is alternative to existing methods for prediction of ground vibration due to heavy vehicle traffic. However, results need to be generalized as present work is valid only for considered data. Comparison of measured and predicted PPV values for training data is shown in Figure 6.

Vibration caused by vibratory roller

The vibratory energy of machines depends on type of compaction. Tables 5 and 6 contains the measurements

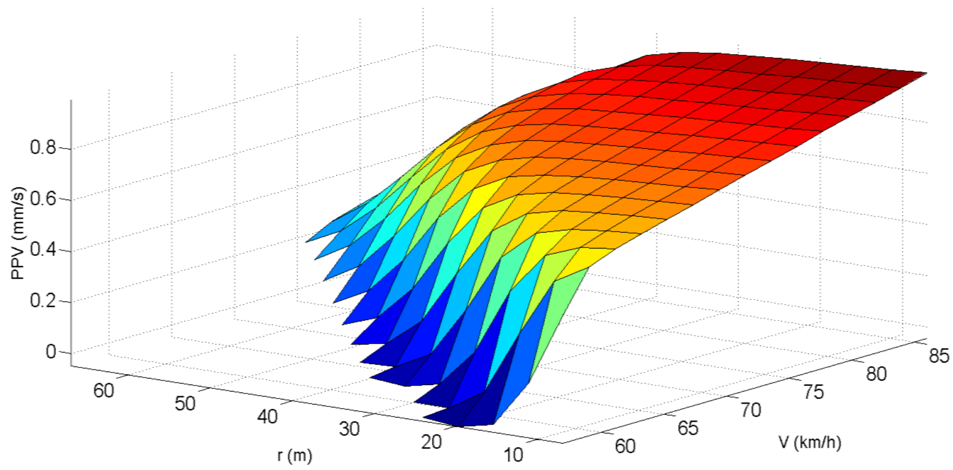

Figure 5. Result of ANFIS model.

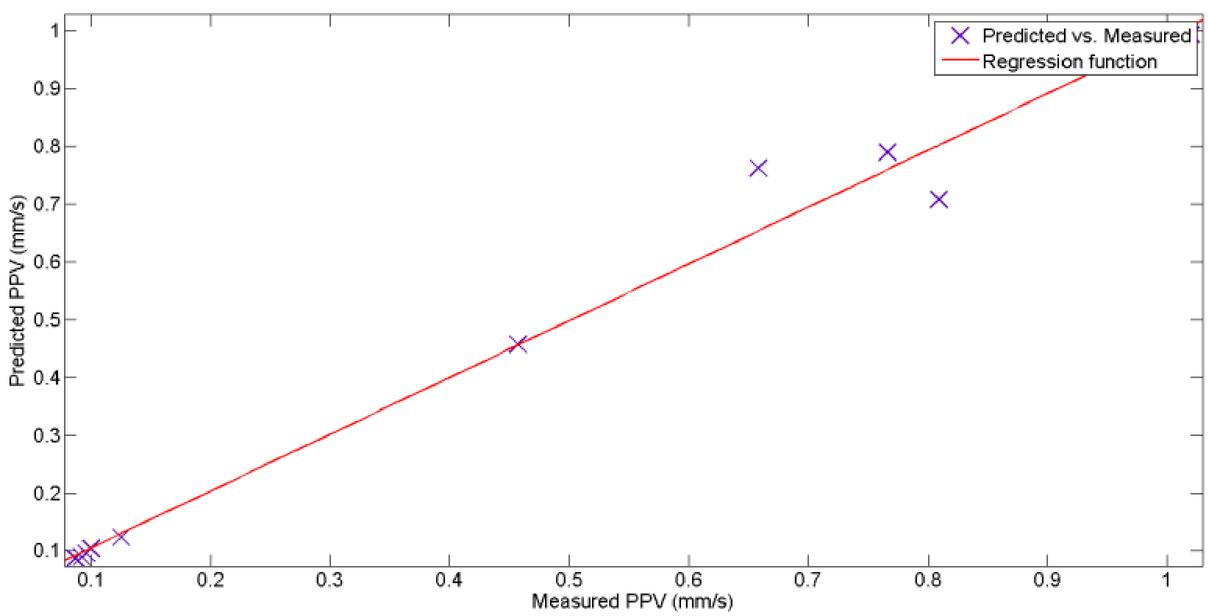

Figure 6. Measured versus predicted PPV values for training data sets.

Table 5. PPV measurement results caused by three types of compaction methods for heritage objects.

Distance (m)	PPV (mm/s) Surface dynamic compaction	PPV (mm/s) Deep dynamic compaction	PPV (mm/s) Static compaction
8.0	3.57	3.51	0.220
8.9	3.28	2.91	0.220
10.7	2.61	1.50	0.311
30.0	2.22	0.93	0.220

of PPV for surface dynamic, deep dynamic and static compaction. Additionally the measurements are obtained on two buildings with different quality of foundations. For each building, type of compaction and various distances

Table 6. PPV measurement results caused by three types of compaction methods for residential objects.

Distance (m)	PPV (mm/s) Surface dynamic compaction	PPV (mm/s) Deep dynamic compaction	PPV (mm/s) Static compaction
5.4	2.01	1.51	0.220
7.1	1.94	1.50	0.220
15.1	0.93	1.26	0.254
16.0	1.02	0.81	0.284

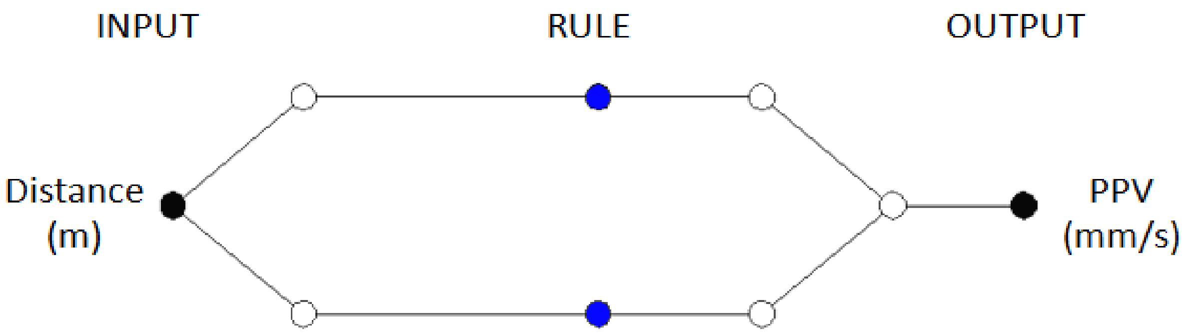

Figure 7. Constructed ANFIS models for prediction of ground vibration caused by compaction.

Table 7. PPV measurements caused by three types of compaction methods.

Number of training data sets	6 x 4
Type	Sugeno
Number of input membership functions	2, Gaussian
Number of output membership functions	2, Constant
Number of rules	2
And method	prod
Or method	probor
Defuzzification method	wtaver
Implication method	prod
Aggregation method	max

from the source of vibrations the PPV were measured. Based on the measurements the simple one parameter ANFIS models were constructed (Figure 7). The PPV value is predicted for two different types of foundations and three types of compaction, therefore six models were constructed with the same structure. Table 7 presents the input data of fuzzy models, which are essential to repeat the calculations.

Results of ANFIS model – vibration caused by vibratory roller

Figure 8 shows the vibration velocity as a function of distance from the source of vibration – based on ANFIS model. Figure 8a shows the graphs for the heritage objects which have generally poorly foundations and have no built-in anti-seismic ties. Graphs on Figure 8b are shown the same physical quantity but for residential objects, which are better quality. A graphical representation of vibration velocity of the distance from the source of vibration indicates that the vibration velocity depends on the type of hardening of soil produced with roller. From the graphs it is evident that surface dynamic compaction and deep dynamic compaction cause almost the same vibration velocity in a small distance from the source of vibration. With increasing distance from the source of vibration surface dynamic compaction leads to

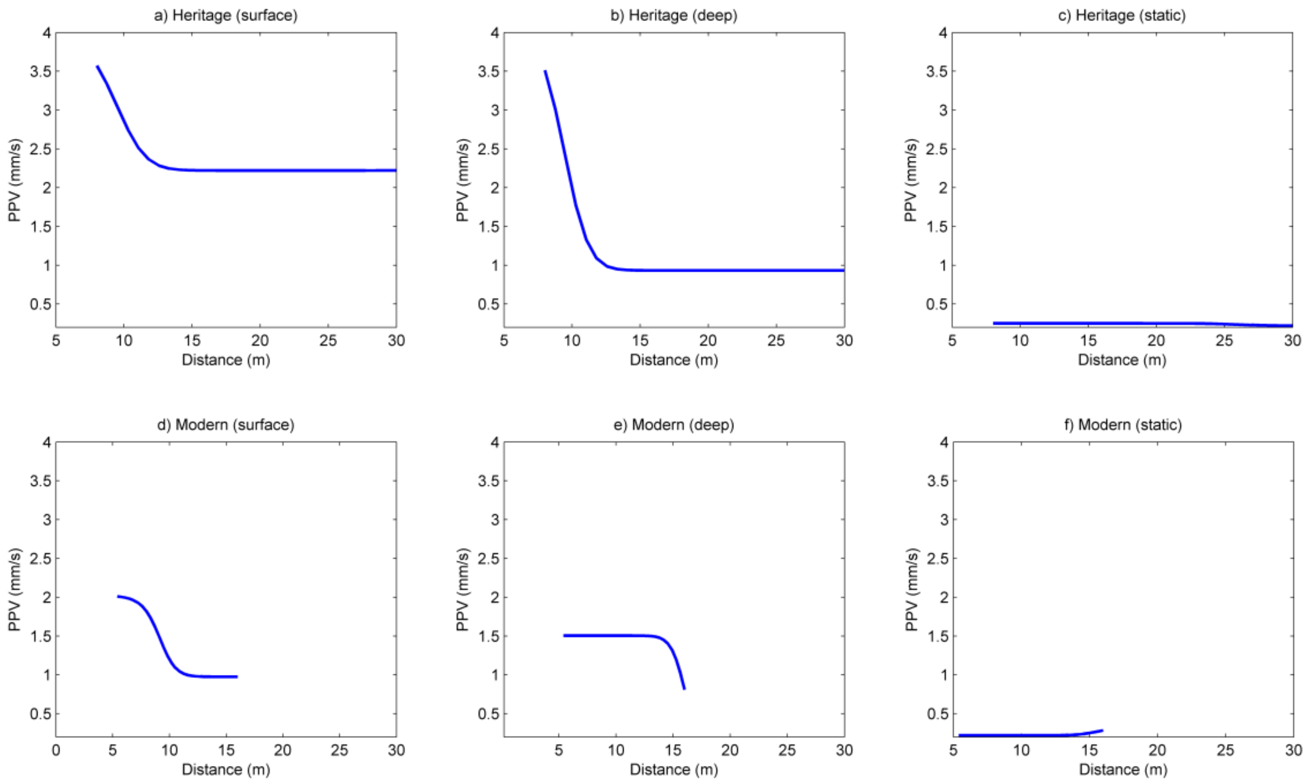

Figure 8. Results of ANFIS model – measuring values which are shown in Tables 5 and 6.

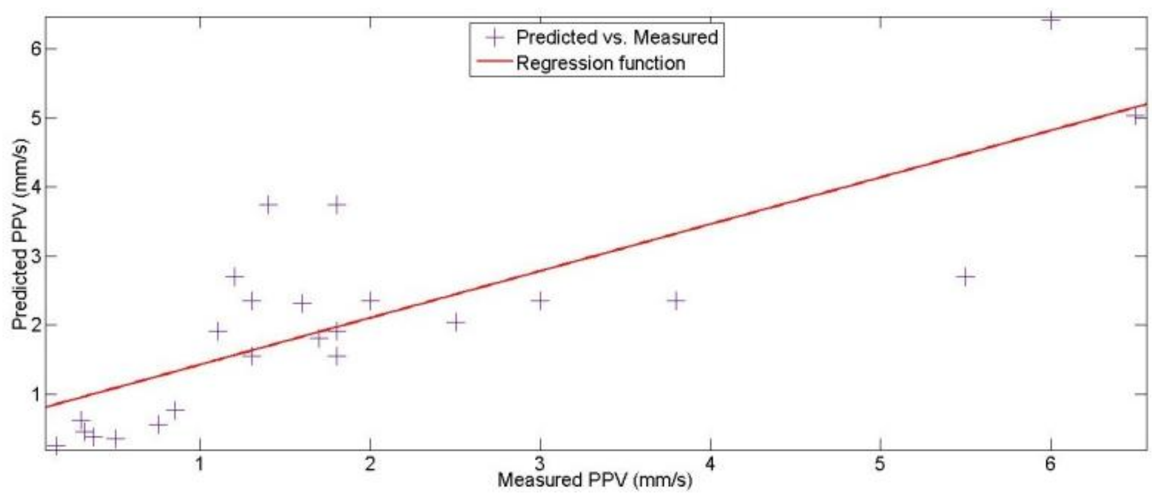

Figure 9. The measured versus predicted ground vibrations due to a road roller activity.

a higher vibration velocity when compared with the deep dynamic compaction. Vibration velocity caused by the static compaction is negligibly small when compared with the vibration velocity induced by surface and deep dynamic compaction. Calculations also confirmed by the fact that the vibration velocity and the distance of the same intensity and the distance of the source are greater then in residential objects. Additionally, we have constructed an ANFIS, based on measurements provided by Achmus et al. (2005). With the developed model we are able to predict the PPV value for any selected distance. Figure 9 shows the measured versus predicted ground vibrations due to a road roller activity.

CONCLUSIONS AND RECOMMENDATION

The measured foundation oscillation velocities presented in Figure 1 correspond very well with the line of the prognostic Equation (3). We can conclude that the prognostic Equation (3) can be used for the preliminary assessment of foundation oscillation velocity within the scope of risk assessment. Based on the calculation with the prognostic Equation (3), the likely value of foundation oscillation velocity is 0.12 mm/s, while the DIN 4150 standard provides an orientation value of 5 mm/s for horizontal components of oscillation velocity. If this value is not exceeded, we do not expect damage to the building and can exclude the likelihood that horizontal oscillations of structural elements would occur on the top floor of the building with the increase of the oscillation amplitude. For vertical oscillation velocities of the ceiling in the building, DIN 4150 provides an orientation value of 8 mm/s. At a frequency of the vibrating roller of 30 Hz there could be a risk of resonance. However, considering that the transfer factor for wooden ceilings $kz \leq 15$ (Funk, 1996), we obtain the maximum oscillation velocity of 1.8 mm/s using the prognostic Equation (4), which means that in no event the guideline value of the standard DIN 4150 is exceeded and no damage is expected to the building. According to the prognostic Equation (4), the measured values of driving, and in some cases of pulling, sheet piling correspond very well with the boundary probability line. The results for pulling sheet piling in a direct vicinity of the measuring point present a border case, a very troublesome one, which is difficult to predict due to the proximity of the source. When planning construction works it is therefore necessary to assess possible effects of vibrations and the resulting risks, and select such building machines whose operation does not affect surrounding buildings or is at least minimized. The measurement of vibrations resulting from heavy trucks has shown that the prognostic Equation (4) sets very strict criteria, which are mostly exceeded in our case.

Data scattering of vibrations is very large, therefore conventional vibration predictors are not able to predict the PPV up to an acceptable limit. Many researchers found out that artificial neural network and neuro-fuzzy technique have superiority in solving problems in which many complex parameters influence the process and results, when process and results are not fully understood. Therefore is very important that experimental data are available. The prediction of ground vibrations due to heavy vehicle traffic is also of this type. Speed of a vehicle and the distance between the measuring point and the moving vehicle are two input parameters for ANFIS model. Built model can be improved with more measurements of ground vibrations. Based on engineering judgment, the proper measurements should be selected for training and checking data sets. Prediction of vibration caused by the dynamic compaction of soils with vibratory rollers are in good agreement with calculations by prognostic Equations (2) and (3). The elaborated method using techniques FIS and model ANFIS can be applied to assesment of vibration of buildings. The results of experiments show, that application of this methods are possible.

Conflict of Interest

The authors have not declared any conflict of interest.

REFERENCES

Achmus M, Kaiser J (2006). Prognose von Bauwerkserschütterungen infolge Ramm- und Vibrationsverdichtungarbeiten. Danube-European conf. Geotech. Eng. 2:723-728.

Achmus M, Kaiser J, Wörden FT (2005). Bauwerkserschütterungen durch Tiefbauarbeiten: Grundlagen, Messergebnisse, Prognosen. Institut für Grundbau, Bodenmechanik und Energiewasserbau, Universität Hannover, Hannover. 61:1-82.

Faravelli L, Yao T (1996). Use of adaptive networks in fuzzy control of civil structures. Computer-Aided Civ. Infrastructure Eng.11(1):67-76.

Funk K (1996). Expertsystem für Lärm- und Erschütterungsprognosen beim Einbringen von Spundbohlen. Mitteilungen des Curt-Risch-Institut für Dynamik, Schall- und Messtechnik der Universität Hannover. 2(96):1-145.

Gokceoglu C, Yesilnacar E, Sonmez H, Kayabasi AA (2004). Neuro-fuzzy model for modulus of deformation of jointed rock masses. Comput. Geotech. 31:375–383. http://dx.doi.org/10.1016/j.compgeo.2004.05.001

Hunaidi O (2000). Traffic vibrations in buildings. construction technology update No. 39, National Research Council of Canada. 39:1-9.

Jang JSR (1993). ANFIS: Adaptive-Network-Based Fuzzy Inference System. IEEE Trans. Syst. Man Cybernetics. 23(3):665-685. http://dx.doi.org/10.1109/21.256541

Kayadelen C, Gunaydin O, Fener M, Demir A, Ozvan A (2009). Modeling of the angle of shearing resistance of soils using soft computing systems. Expert Syst. Appl. 36:11814-11826. http://dx.doi.org/10.1016/j.eswa.2009.04.008

Khandelwal M (2012). Application of an expert system for assessment of blast vibration. Geotech. Geol. Eng. 30:205-217. http://dx.doi.org/10.1007/s10706-011-9463-4

MATLAB version 7.10.0. (2010). Natick, Massachusetts: The MathWorks Inc.

Philipps G, Stollhoff F, Wieck J (2010). Die vorsorgliche Beweissicherung im Bauwesen: Reihe begründet von Günter Zimmermann. Fraunhofer IRB Verlag. pp. 33-66.

Provenzano P, Ferlisi S, Musso A (2004). Interpretation of a model footing response through an adaptive neural fuzzy inference system. Comput. Geotech. 31:251-266. http://dx.doi.org/10.1016/j.compgeo.2004.03.001

Rangel JL, Iturraran-Viveros U, Ayala AG, Cervantes F (2005). Tunnel stability analysis during construction using a neuro-fuzzy system. Int. J. Numer. Anal. Methods Geomech. 29:1433–1456. http://dx.doi.org/10.1002/nag.463

Rumelhart DG (1986). Learning representations by back-propagating errors. Nature 323:533-536. http://dx.doi.org/10.1038/323533a0

Sugeno M (1985). Industrial applications of fuzzy control. Elsevier Science pub. 1-18.

Watts GR (1990). Traffic induced vibrations in buildings. Research Report 246, Transport and Road Research Laboratory, Department of Transport, UK. 246:1-31.

International Journal of Physical Sciences

Related Journals Published by Academic Journals

- *African Journal of Pure and Applied Chemistry*
- *Journal of Internet and Information Systems*
- *Journal of Geology and Mining Research*
- *Journal of Oceanography and Marine Science*
- *Journal of Environmental Chemistry and Ecotoxicology*
- *Journal of Petroleum Technology and Alternative Fuels*